Missouri State University

BearWorks

MSU Graduate Theses

Spring 2022

Elucidating the Role of Hemodynamic Force in Regulating the Attachment of Vascular Smooth Muscle Cells (VSMCS) to Maturing Vessels During Mouse Embryonic Development

Israt Jahan
Missouri State University, Israt017@live.missouristate.edu

As with any intellectual project, the content and views expressed in this thesis may be considered objectionable by some readers. However, this student-scholar's work has been judged to have academic value by the student's thesis committee members trained in the discipline. The content and views expressed in this thesis are those of the student-scholar and are not endorsed by Missouri State University, its Graduate College, or its employees.

Follow this and additional works at: https://bearworks.missouristate.edu/theses

 Part of the Developmental Biology Commons

Recommended Citation

Jahan, Israt, "Elucidating the Role of Hemodynamic Force in Regulating the Attachment of Vascular Smooth Muscle Cells (VSMCS) to Maturing Vessels During Mouse Embryonic Development" (2022). *MSU Graduate Theses*. 3737.
https://bearworks.missouristate.edu/theses/3737

This article or document was made available through BearWorks, the institutional repository of Missouri State University. The work contained in it may be protected by copyright and require permission of the copyright holder for reuse or redistribution.
For more information, please contact bearworks@missouristate.edu.

ELUCIDATING THE ROLE OF HEMODYNAMIC FORCE IN REGULATING THE ATTACHMENT OF VASCULAR SMOOTH MUSCLE CELLS (VSMCS) TO MATURING VESSELS DURING MOUSE EMBRYONIC DEVELOPMENT

A Master's Thesis

Presented to

The Graduate College of

Missouri State University

In Partial Fulfillment

Of the Requirements for the Degree

Master of Science, Biology

By

Israt Jahan

May 2022

Copyright 2022 by Israt Jahan

ELUCIDATING THE ROLE OF HEMODYNAMIC FORCE IN REGULATING THE ATTACHMENT OF VASCULAR SMOOTH MUSCLE CELLS (VSMCS) TO MATURING VESSELS DURING MOUSE EMBRYONIC DEVELOPMENT

Biology

Missouri State University, May 2022

Master of Science

Israt Jahan

ABSTRACT

Blood vessel maturation is characterized by the recruitment and attachment of vascular smooth muscle cells (vSMCs) around immature blood vessels, which ultimately form the tunica media. Improper maturation can lead to vascular birth defects ranging from minor birthmarks to lethal brain aneurysms. Previously, our lab demonstrated that hemodynamic force plays an important role to regulate vSMCs recruitment from neighboring low-flow to high-flow vessels followed by the attachment of these vSMCs to the high-flow vessels. To understand the reason for the preferred attachment of vSMCs to high-flow vessels, instead of low-flow vessels, I hypothesize that hemodynamic force modulates the expression of extracellular matrix genes to promote the deposition of a thick basement membrane around the immature high-flow vessels to increase its adhesiveness to migrating vSMCs. To test this hypothesis, I utilized an extraembryonic tissue called the yolk sac, which is a thin/transparent membrane only comprised of simple blood vessels, and I compared gene expression differences by qPCR between yolk sac tissues under normal blood flow with those having reduced blood flow. I found that there is a decrease in *matrix metalloproteinase-9 (MMP-9)* expression in high-flow vessels as compared to low-flow vessels. My data support our hypothesis as lowering MMP9 should promote deposition of a thicker basement membrane, thus enhancing the attachment of vSMCs to high-flow vessels.

KEYWORDS: vascular smooth muscle cells, vessel maturation, hemodynamic force, extracellular matrix genes, basement membrane.

ELUCIDATING THE ROLE OF HEMODYNAMIC FORCE IN REGULATING THE ATTACHMENT OF VASCULAR SMOOTH MUSCLE CELLS (VSMCS) TO MATURING VESSELS DURING MOUSE EMBRYONIC DEVELOPMENT

By

Israt Jahan

A Master's Thesis
Submitted to the Graduate College
Of Missouri State University
In Partial Fulfillment of the Requirements
For the Degree of Master of Science, Biology

May 2022

Approved:

Kyoungtae Kim, Ph.D., Thesis Committee Chair

Paul L. Durham, Ph.D., Committee Member

Christopher Lupfer, Ph.D., Committee Member

Julie Masterson, Ph.D., Dean of the Graduate College

In the interest of academic freedom and the principle of free speech, approval of this thesis indicates the format is acceptable and meets the academic criteria for the discipline as determined by the faculty that constitute the thesis committee. The content and views expressed in this thesis are those of the student-scholar and are not endorsed by Missouri State University, its Graduate College, or its employees.

ACKNOWLEDGEMENTS

I would like to thank Dr. Ryan Udan for mentoring me for the last two years, guiding me in my research, being considerate, and teaching me all the things hands-on. I am thankful to Dr. Kyoungtae Kim, the Chairman of my thesis committee, Drs Paul L Durham, and Christopher Lupfer for helping me during the last portion of my thesis. I am thankful to my lab mates Shamita Gazi, Justin Galisim, and all the other lab members for their support in my project. I am very thankful to the Department of Biology of Missouri State University for providing enormous facilities to complete my graduate studies here.

I am very much grateful to my baby Drik Hasan for their continuous support. Without their endless support, it would not be possible for me to pursue my degree.

I dedicate this thesis to my loving son Drik

TABLE OF CONTENTS

Introduction	Page 1
Role of the Cardiovascular System During Development	Page 1
Relevance to Human Health	Page 2
Current Views on Cardiovascular Development	Page 4
Development of the Mouse Heart	Page 4
Development of the Mouse Vasculature	Page 5
Angiogenesis	Page 7
Developmental Vascular Remodeling	Page 9
Artery/Venous Specification	Page 11
Vascular Maturation	Page 12
The Role of Hemodynamic Force in Regulating Vascular Maturation	Page 14
Hypothesis	Page 15
Materials and Methods	Page 17
Mouse Husbandry	Page 17
Embryo Collection and Genotyping	Page 18
qPCR	Page 20
Data Analysis	Page 25
Cryosectioning	Page 25
Immunostaining	Page 25
Imaging	Page 26
Results	Page 28
Discussion	Page 36
References	Page 41
Appendix: IACUC Approval	Page 45

LIST OF TABLES

Table 1. Primers used in the study Page 22

Table 2. Antibodies used in the study Page 26

Table 3. CT values for ECM and ECM related genes in control and experimental samples in the qPCR study Page 30

LIST OF FIGURES

Figure 1. Change in ECM gene expression Page 31

Figure 2. Change in ECM remodeling gene expression Page 32

Figure 3. Dorsal Aorta cross-section of normal-flow embryos with collagen IV Page 33

Figure 4. Dorsal Aorta cross-section tissue of normal-flow embryos with MMP-9 Page 34

INTRODUCTION

The cardiovascular system is the first functional organ system that starts working at the beginning of the fourth week of embryonic development in humans (Mathew, Bordoni, 2021). In mammals, the cardiovascular (CV) system is composed of the heart and blood vessels. Its major role is to enable gas exchange, supply nutrients, and remove waste products, but it also plays a role in endocrine signaling and serves as a conduit for the movement of immunological cells throughout the body (Udan, Culver, & Dickinson, 2013). At the center of the CV system is the heart. The heart is comprised of left and right atria and left and right ventricles. Through coordinated contractions, blood is efficiently pumped to the lungs or to the body via the vasculature. The right side of the heart receives deoxygenated blood from the body and transfers it to the lungs to be oxygenated. The left side of the heart receives the oxygenated blood from the lungs and transmits it to the rest of the body through the vasculature. The vasculature is a complex system comprised of a hierarchy of different vessel subtypes (from arteries to arterioles, capillaries, venules, and veins). Arterial walls are thicker and more elastic than other vessels to withstand the high blood pressure, whereas veins are less elastic and less muscular due to the presence of reduced blood pressure. Capillaries, which have lower blood flow and are much smaller, facilitate the diffusion of gases and nutrients. Collectively, the heart and vasculature are highly organized structures that are required for embryonic/fetal survival.

Role of the Cardiovascular System During Development

The CV system forms during embryonic development. When a mammalian embryo embeds into the uterus, it is still devoid of a CV system, but eventually, it develops one to meet

increasing metabolic demands of the embryo. Through several cellular and molecular mechanisms, some known and some unknown, the CV arises. However, there are some situations where the CV system does not form, or it does not form properly, and this can be disadvantageous to human health.

Relevance to Human Health

The way in which defective CV development can impact the health of people is through the formation of congenital heart and vascular defects. For example, there are a wide variety of congenital heart defects (CHDs) that affect the size of the heart or thickness of the heart tissue. They can also affect the separation of the chambers of the heart or the fusion of the vessels that are directly connected to the heart (Suluba, Shuwei, Xia, & Mwanga, 2020). Those defects can impair normal blood flow and can affect further heart development. Children born with CHDs may develop some complications like developmental delay, repeated respiratory infection, pulmonary hypertension, and heart failure while other children may not experience cardiovascular issues until much later in adulthood.

Another type of defect in the development of the CV system is congenital vascular anomalies (CVAs). CVAs can affect different vascular structures like arteries, veins, lymphatic vessels, and capillaries separately, or sometimes involve two or more vascular structures that are known as mixed lesions (Eerola, Boon, Mulliken 2003). Though less prevalent, there are a wide variety of these anomalies. For example, arterial-venous fistulas, hemangiomas, and congenital aneurysms. Clinical presentations depend on the type of malformation, location, size, and relationship with other structures and can be named according to the affected structure. Arteriovenous (AV) fistulas are an abnormal connection between an artery and a vein without an

intervening capillary bed that can lead to venous hypertension, arterial insufficiency, high cardiac output failure, and hemorrhage (Jayroe, 2020). Children can be born with this condition in different locations of the body including pulmonary, hepatic, aortocaval, coronary, and carotid-cavernous vessels (Reynolds, Lanzino, & Zipfel, 2017). Despite the frequent occurrence of these conditions, the etiology of AV fistulas is not well understood.

A congenital aneurysm is a rare case that can occur where infants are born with weak vessels having thin layers of tissues. Weak or thin-walled vessels are prone to hemorrhaging, and in some cases, they only cause birthmarks, but in other cases, it can involve larger vessels that are prone to rupture later in life. In cerebral aneurysms, most of the aneurysms are located along the bifurcation of the Circle of Wills which can cause subarachnoid hemorrhaging (SAH) after rupture. A rupturing aneurysm is one of the major causes of atraumatic SAH in children, and approximately 65% of patients present with rupture at the time of diagnosis (Amacher & Drake, 1975). Sudden thunderclap headache, loss of consciousness, seizure, and coma are the common presenting features of a ruptured aneurysm, and some patients may present with recurrent bleeding episodes. The overall mortality rate of children after a ruptured aneurysm is 13% to 34% (Levy, 2021).

To understand how these vascular anomalies such as congenital aneurysms arise, we first must learn the fundamental mechanisms governing the growth, development, and maturation of these vessels. This will allow us to elucidate important mechanisms and molecules needed for proper growth of the vasculature, and this information may also allow us to develop therapeutic approaches to repair improperly developed vessels. Knowledge about vascular maturation is also important in utilizing tissue-engineering approaches (Jain, 2003). Every year many people need organ transplantation but one of the major impediments in organ transplantation is finding an

appropriately matched donor. The problem in donor finding can be solved by designing artificial organs. One of the challenges of designing artificial organs is developing a functional 3D vasculature to regulate blood flow to the organ. Uncovering the unknown information about cellular, molecular, and biochemical cues of blood vessel formation can help in designing a functional vasculature.

Current Views on Cardiovascular Development

The early post-implantation mammalian embryo lacks a CV system because it is supported by simple diffusion of gas and molecules from the maternal tissues. However, as the embryo increases its size, it will need a functional circulatory system (Udan, Vadakkan, & Dickinson, 2013). How does the cardiovascular system form?

Development of the Mouse Heart

Much of what we know about heart development has been elucidated in model organisms such as the mouse. In the mouse, heart development begins with a subset of lateral plate mesoderm, referred to as cardiogenic mesoderm, found on the left and right sides of the developing embryo (Paige, Plonowska, Xu, & Wu, 2015). This cardiogenic mesoderm coalesces into two tubes of tissues. Each tube is comprised of an inner layer (endocardium) and outer layer (myocardium), and these tubes ultimately fuse together to form one unit referred to as the heart tube. This heart tube will continue to develop by a process of looping, ballooning, septa growth, and valve growth (Anderson, Webb, Brown, Lamers, & Moorman, 2022). This results in a four-chambered heart that ultimately becomes connected to the following vessels (aorta and vena cava, and pulmonary artery and vein).

Development of the Mouse Vasculature

Vessel development in the mouse begins slightly earlier than the heart. It occurs initially at several sites (the yolk sac, the embryo, and the chorion/placenta). Vessel development begins by the process of vasculogenesis. Vasculogenesis is a *de novo* process where endothelial cell precursors (angioblasts) assemble and form a new functional vessel. This process is not limited only during embryogenesis, but it can occur at different stages from embryogenesis to adulthood. To start vasculogenesis, the angioblasts must first be specified. Regardless of the location of vasculogenesis, all angioblasts form from a subset of mesoderm. One of the important signaling molecules that helps to specify angioblasts from the mesoderm is the vascular endothelial growth factor (VEGF) (Ferrera, 2000). VEGF binds to a subset of mesoderm via its cognate receptor, vascular endothelial growth factor receptor 2 (VEGFR2). VEGF has been shown to be important in specifying angioblasts, and hence endothelial cells. This is based on evidence revealing that removal of VEGF signaling impedes endothelial cell formation (Shalaby et al., 1995).

In the mouse embryo, the angioblasts that are specified by VEGF arise from a subset of mesoderm that is actively migrating through the primitive streak. These cells ingress between the epiblast and primitive endoderm layers through a circular cavity known as a primitive pit. Eventually, these cells arrive at the embryo proper (where the intraembryonic vessels form), as well as the extraembryonic region of the embryo (where the yolk sac vessels form).

The yolk sac is the first location where vasculogenesis takes place. In the yolk sac, angioblasts are found in close proximity to hematopoietic precursor cells. Here, the angioblasts surround the hematopoietic precursor cells and form several clusters of cells called blood islands (Udan, Culver, et al., 2013). These blood island cells condense (allowing angioblasts to adhere to each other) and the angioblasts between neighboring blood islands adhere with one another. This

ultimately results in a network of interconnected tubes of angioblasts (now called endothelial cells) that surround the hematopoietic precursor cells that are referred to as primitive blood cells (Majesky, 2018; Patan, 2004; Risau & Flamme, 1995). Here the network is called a capillary plexus. During this process, the tubes become lumenized and filled with plasma.

Shortly after extraembryonic vessel formation in the mouse embryo at embryonic day (E) 7.3, the dorsal aorta starts to form from the intraembryonic angioblasts as two separate vessels that later fuses in the midline to form one single vessel (Collart et al., 2021). There are some differences between extraembryonic and intraembryonic vessel formation. During intraembryonic vascular formation, the new vessels do not surround hematopoietic precursor cells, as in the yolk sac vessels. However, in a small paraaortic region, and at a slightly later stage, some of the blood vessel endothelial cells have hemogenic potential, as they have been shown to be hemogenic endothelium, which are cells capable of giving rise to primitive blood cells (Garcia, Lopez, Larin, & Larina, 2015). However, a majority of early embryonic erythropoiesis occurs almost exclusively at the yolk sac.

One of the last steps before the onset of angiogenesis in mouse embryos is the connection of the extraembryonic/yolk sac vasculature and the intraembryonic vasculature with each other as well as to the heart. This occurs at E8.0 and is quickly followed by the initiation of heart contractions at E8.25. During this time, the force of plasma flow allows for the primitive blood cells in the yolk sac vessels to enter circulation, resulting in blood moving into the heart and through the dorsal aortae. Thus, a circulatory connection develops between extraembryonic and intraembryonic tissues.

Angiogenesis

Angiogenesis is the formation of vasculature from pre-existing vasculature. This process is not only limited to developing embryos but can occur in different stages of life in response to hypoxia, wound healing, and tumor growth. In adult life, this process needs to be regulated tightly because both overproduction and reduced production of blood vessels can be associated with diseased conditions. Tissue hypoxia can activate the cellular production of VEGF and cytokines that are the key regulators to start angiogenesis. VEGF together with NOTCH signaling can exert diverse biological effects like endothelial cell differentiation, migration, maintaining vascular diameter, and so on. In the mouse embryo, angiogenesis starts approximately at E8.5 from the newly formed primitive vascular plexus (Lucitti et al., 2007). Angiogenesis may occur via four distinct mechanisms such as sprouting, fusion, intussusception, and regression.

The predominant mechanism governing angiogenesis is a process called sprouting. Sprouting angiogenesis is a process where specialized endothelial cells (found within functioning vessels) grow a new vessel (called a sprout) to create a new tube that ultimately connects to another vessel. When this is repeatedly done, it forms a new functional vascular network. To start sprouting, endothelial cells turn into two distinct phenotypic forms known as tip cells and stalk cells; each having special functional characteristics. Endothelial cells which are exposed to the highest amount of VEGF through its receptor (Vegfr2) turn into tip cells. Tip cells are in the distal end of the sprouting vessel and can migrate due to the presence of lamellipodia and filopodia extensions. Due to VEGF signaling, tip cells upregulate expression of the notch ligand, delta like ligand-4 (Dll4), which plays an important role in specifying stalk cells in neighboring cells, as well as proteinases that promote sprouting into the surrounding tissue. Through Dll4

induction of notch signaling in neighboring cells, the identity of those neighboring cells become stalk cells (D'Alessio, Moccia, Li, 2015). These endothelial stalk cells have fewer filopodia, but a higher proliferative capacity, allowing a new vessel to extend outward into the tissue. In addition, stalk cells stabilize the new sprout by expressing adherens junction proteins and creating the lumen in the new vessel. To ensure stalks cells do not become tip cells, the elevated notch signaling within the stalk cells results in a decrease in VEGFR2 expression. This reduces the cellular response of stalk cells to VEGF. After specification of the tip cell and the stalk cells, vessel outgrowth occurs perpendicularly due to the release of soluble fms like tyrosine kinase (FLT1) from the stalk cells, which causes a steepness of VEGF gradient and enhances proliferation of stalk cell, so that the vessel grows outwardly.

Fusion is another process of angiogenesis where vessels combine. This can occur by joining two sprouts together in a process called anastomosis or by fusing two parallel blood vessels together. Though the exact mechanism of the latter process is not known, in the former process, macrophages can secret VEGF-C, which promotes the conversion of two contacting tip cells to form new stalk cells, resulting in the fusion of two sprouted blood vessels (Tamella, Zarkada, et al., 2011).

Another mechanism to either create new vessels, or to change the branching angles of vessels is called intussusception or splitting angiogenesis. This process is essentially the opposite of fusion. Intussusception occurs by the formation of intraluminal vascular pillars that invaginate into a capillary lumen. Though this form is the least common, this process has been observed in different species and in different organs/tissues like the lung, chorioallantoic membrane, kidney, heart, and endometrium (Udan, Culver, et al., 2013). According to morphological characteristics, intussusception can be divided into three types such as intussusceptive microvascular growth,

intussusceptive arborization, and intussusceptive branching remodeling. Intussusceptive arborization can help in vascular remodeling by creating new vessels, whereas intussusceptive branching remodeling changes the angles of blood vessel branches.

The last mechanism of angiogenesis, vascular regression, is utilized to remove supernumerary vessels. It is the systemic pruning of unnecessary vessels to create a stable vascular network that is important to maintain vascular homeostasis. Various factors including reduced shear stress and decreased hypoxia can cause vascular pruning by inducing anti-angiogenic signaling (Ricard & Simons, 2015).

In early development, newly formed blood vessels are mostly equivalent in diameter. However, they eventually develop into different diameters to form a hierarchy. This occurs by the process of vascular remodeling, which utilizes some of the processes of angiogenesis.

Developmental Vascular Remodeling

Developmental vascular remodeling is a process that leads to the correct branching and growth (diameter increase) of vessels to form a hierarchy of large-diameter proximal vessels (located closer to the heart) that branch into small-diameter distal vessels (located away from the heart). This hierarchy is crucial in directing blood to tissues and to facilitate diffusion in small capillaries while maintaining the correct dimensions that allow for the heart to physically pump blood through the body.

Vascular remodeling takes place in the mouse between E8.5-9.5 (Armulik, Abramsson, & Betsholtz, 2005), and any impairment of remodeling halts further development of embryos since underdeveloped vessels will fail to provide oxygen and nutritional support to the tissues). Besides molecular cues, it has long been known that hemodynamic force plays a very critical

role in vascular remodeling, as disruptions in normal blood flow in mouse embryos result in a failure for the blood vessels to properly remodel. For instance, functional mutation of *myosin light chain 7 (Myl7 / Mlc2a*), which is a structural component of atrial myofibril, can disrupt the ability of the atria of the heart to contract, only allowing the ventricles to pump blood throughout the embryo. As a result, this reduces the hemodynamic force that the blood vessels of the embryo are exposed to, which results in impairment in vascular remodeling at E9.5 (Lucitti et al., 2007). To prove that impaired vascular remodeling was specifically caused by a reduction in hemodynamic force, and not due to inadequate oxygenation of the tissue, Lucitti *et al.* compromised remodeling in a different way, by experimentally removing erythroblasts from cultured mouse embryos to produce low-hematocrit embryos (Lucitti et al., 2007). This lowers the viscosity of the plasma, which in turn reduces the hemodynamic force that the vessels are exposed to. Then, the researchers were able to rescue the vascular remodeling defect in the low-hematocrit embryos by injecting hetastarch into the vessels. Since hetastarch does not provide oxygenation to the tissues but does increase plasma viscosity, the experiment demonstrated that the hemodynamic force exerted by flow was essential for vascular remodeling.

To understand how hemodynamic force accounts for the changes in vessel diameter that occur during remodeling, another study was performed using live confocal imaging to visualize vessel diameter increases (Udan, Vadakkan, et al., 2013). In this study, the dynamics of vessel remodeling were visualized by comparing the proper remodeling that occurs in normal-flow mouse embryos (wild type) versus the abnormal remodeling that occurs in reduced-flow ($Myl7^{-/-}$) mouse embryos. Results from that study revealed that normal-flow mouse embryos exhibit a variation of hemodynamic force throughout the vascular bed (in this case the yolk sac tissue). Vessels that have high blood flow (high hemodynamic force) and tend to be located closer to the

heart (proximal) then fuse with neighboring vessels to create larger-diameter vessels. Also, the proximal vessels continue to grow larger, as endothelial cells can migrate collectively towards the proximal vessel. This further increases diameter of the proximal vessel, while diminishing vessel diameter at vessels located farther away from the heart and downstream (distal vessels). Interestingly, hemodynamic force is required for these dynamic cell and tissue movements, as reduced-flow embryos lack the ability for vessels to fuse and for the endothelial cells to migrate towards proximal vessels. Therefore, it is obvious that hemodynamic force plays a crucial role in vascular remodeling.

Artery/Venous Specification

Before vascular remodeling occurs, the vessels begin to display differences based on their proximity and location to the heart. Vessels that pump blood away from the heart become arteries, and those that move blood toward the heart become veins. There is much experimental evidence to show that arterial and venous identities are specified before remodeling. Several genetic mechanisms may be involved including Notch signaling and Ephrin/Eph receptor signaling (Lawson, Scheer, Pham, Kim, & Chitnis, 2001). In the mouse yolk sac vessels, presence of EphrinB2 determines arterial endothelial cell and EphrinB4 determines venous endothelial cells (Fang & Hirschi, 2019). Also, Notch and their downstream effector molecules are required for arterial specification, whereas venous specification does not require Notch signaling. However, other evidence suggests that these identities are not necessarily irreversible, as they have to be reinforced/maintained during vascular remodeling (Oliver & Srinivasan, 2010). For example, Le Noble et. al showed that ligation (blockage of blood flow) in the right vitelline artery of chick embryos resulted in a downregulation of several arterial markers (le

Noble et al., 2004) whereas, in mouse embryos, cessation of flow only results in a downregulation of some arterial markers but not others (Jones, Yuan, Breant, Watts, & Eichmann, 2008). The consensus within the field, from studies such as these, is that hemodynamic force is not required for arterial/venous specification, but instead is required for maintaining expression or arterial or venous markers/fates (Buschmann et al., 2010; Campinho, Vilfan, & Vermot, 2020). Once specified, arteries can adopt structural differences than veins such as a thicker layer of surrounding tissue while veins can adopt a larger diameter than arteries and the presence of valves.

Vascular Maturation

After vessel hierarchy forms, the next step is for the vasculature to become surrounded by extra layers of cells. In E9.0 mouse embryos, the vasculature is just a single-cell layer of endothelial cells, but in the mature embryo, fetus, and adult, vessels can form multiple layers in a process called vascular maturation. Vascular maturation occurs by the recruitment and attachment of mural cells around the newly remodeled endothelial layer. Mural cells can be either vascular smooth muscle cells (vSMCs) or pericytes. Pericytes usually cover micro vessels like capillaries and vSMCs deposit around large diameter vessels as a tissue layer. A mature vasculature usually contains three layers of tissues, such as the tunica intima, tunica media, and tunica adventitia. The tunica media is the middlemost layer formed by the deposition of vSMCs around an immature blood vessel which is crucial to maintain vascular tone and integrity. There is also an outer layer referred to as a tunica adventitia. It is comprised of connective tissues cells that deposit an extracellular matrix, provide elasticity, and support to the vessel, and allow the vessels to connect to other tissues. Interestingly, the existence and number of layers vary

depending on the vessel subtype. Arteries have a thick tunica media to withstand with large pressure force generated by transporting oxygenated blood throughout the body. The tunica media of the vein is thinner than arteries and capillaries (the latter being usually devoid of tunica media).

Though vascular maturation has been studied for many years, queries regarding the molecular mechanisms of this process remains unclear. It was long known that during maturation, endothelial cells secret platelet-derived growth factor b (PDGFB) which is a key regulatory molecule for vSMC recruitment and proliferation (Lindblom et al., 2003). But new studies suggest that instead of recruitment, PDGFB acts to enhance the proliferation of vSMCs only. It has been observed that any mutation in PDGFB reduces the total number of vSMCs, but available vSMCs are still have the capability to recruit to the vessel (French, Creemers, & Tallquist, 2008). So, there must be some other mechanism that regulates vSMCs recruitment. Upon recruitment, vSMCs undergo reciprocal signaling by releasing AGPT1 (Angiopoietin1) to activate the TEK receptor in endothelial cells, which is thought to activate the endothelial expression of adhesion molecules to promote vessel stability. Stabilization of immature vessels make them leak resistant. Transforming growth factor β 1(TGFβ1) is another important factor of vessel maturation that is activated after vSMC-EC interaction. TGFβ1 promotes vascular maturation by promoting extracellular matrix (ECM) formation and by initiating differentiation of mesenchymal cells into vSMCs. Though these signaling molecules seem to play a role in vessel stability and vSMC-EC attachment, it is not clear whether they play a role in controlling the extent of vSMC coverage in different vessels of the hierarchy. Part of the mechanism for understanding the control of this hierarchical difference in tunica media coverage was elucidated in the Udan lab (Padget, Mohite, et al., 2019).

The Role of Hemodynamic Force in Regulating Vascular Maturation

An interesting observation regarding the regulation of vascular maturation is the differences in vSMC coverage throughout the vascular hierarchy. For example, proximal arteries of the developing mouse yolk sac contain the highest vSMC coverage, whereas, extent of coverage diminishes gradually in proximal veins and capillaries (Padget, Mohite, et al., 2019). This difference provides the first clue that hemodynamic force may be responsible for regulating the extent of vSMC coverage, as these different vessels of the yolk sac have a matching level of hemodynamic force (Udan, Vadakkan, et al., 2013). Specifically, proximal arteries have the highest hemodynamic force and greater amount of vSMCs coverage. Whereas capillaries have the lowest vSMCs coverage and the lowest hemodynamic force. To determine whether hemodynamic force is required for vascular maturation, Padget *et al.* sought to determine if reduction of hemodynamic force (in *Myl7*$^{-/-}$ mutant embryos/yolk sacs) impairs maturation (Padget, Mohite, et al., 2019). Indeed, reduction of hemodynamic force results in a reduction of vSMC coverage, including in the proximal arteries of the yolk sac, as well as the dominant intraembryonic vessel, the dorsal aortae. To determine the cellular mechanism of this diminished vSMC coverage, Padget *et al.* revealed that hemodynamic force does not alter the ability of the vSMCs to proliferate or differentiate and thus, there was no change in the total number of vSMCs. Instead, vessels exposed to high-hemodynamic force (high-flow vessel) promote the recruitment and attachment of unattached/migratory vSMCs from neighboring low-flow capillaries. Thus, hemodynamic force is an upstream signal controlling the extent of vSMC coverage and hence the tunica media formation. What remains unknown are the molecular mechanisms governing how the unattached/migratory vSMCs recruit to the high-flow vessels

and how they subsequently attach to the high-flow vessels instead of the low-flow vessels that they encounter along their journey.

Hypothesis

Though we now know that hemodynamic force is required to regulate the extent of vSMC coverage, we still do not know the molecular mechanisms governing the recruitment and attachment of vSMCs to high-flow vessels. The premise of my thesis is to better understand the molecular mechanisms specifically governing why migrating/unattached vSMCs attach to the high-flow vessels, while avoiding attachment to low-flow vessels. I propose that to high hemodynamic force on blood vessel regulates endothelial expression of several genes to control vSMCs attachment. This concept is described in the following hypothesis.

If hemodynamic force modulates expression of extracellular matrix (ECM) and ECM remodeling genes that promote deposition of a thick basement membrane around immature high-flow vessels, then this will increase its adhesiveness to migrating vSMCs.

How (molecularly) does flow/force affects ECM expression or deposition? I posit that the endothelium of high-flow vessel causes some change in protein expression that increases its adhesiveness to vSMCs. There are several candidate genes that may be involved in promoting ECM formation in high-flow vessels. This can occur in two ways: 1) hemodynamic force regulates endothelial expression of ECM genes, or 2) hemodynamic force regulates endothelial expression of genes that regulate ECM deposition. For example, in the first way, there are several ECM proteins like *collagen, laminin, fibronectin, perlecan*, and *nidogen*. Hemodynamic force may upregulate the expression of these ECM proteins resulting in a thicker ECM. Considering that vSMCs express integrin proteins, which are transmembrane proteins that anchor

cells to the ECM, then tissues that have a thicker ECM will more likely adhere to vSMCs (Yousif, Russo, 2013). In the second way, ECM gene expression may not be altered, but basement deposition could still be affected by modulating *matrix metalloproteinase* (*MMP*) and *tissue inhibitor of matrix metalloproteinase* (*TIMP*) gene expression. During embryogenesis, *MMPs* and *TIMPs* play a balancing act at promoting ECM degradation or preventing ECM degradation by inhibiting *MMP* activity, respectively. Due to the opposing effects of *MMPs* and *TIMPs*, I posit that high-flow blood vessels may downregulate *MMPs* and upregulate *TIMPs* expression to promote formation of a thicker ECM (or basement membrane of the endothelium). An opposite expression pattern might be found in low-flow vessels. If this occurs, this may explain the difference in adhesiveness of vSMCs to different vessels of the hierarchy.

MATERIALS AND METHODS

Mouse Husbandry

Mice were accommodated in the Missouri State University Temple Hall vivarium and this project was approved by the Institutional Animal Care and Use Committee (Breeding Protocols: #18-018.0 [November 2017], #2020-21 [October 2020]; Experimental Protocols: #18-019.0 [November 2017], #2020-22 [October 2020] see appendix). The National Institute of Health's animal care and use guidelines were followed when caring for mice. Mice were kept in either an Ancare standard mouse cage or a standard rat cage with either a maximum of 4 mice per mouse cage or 10 mice per rat cage. The rat cage also provided more space for movement and enrichment (mouse wheel), while other forms of enrichment were provided in the mouse cages. Animals were housed in a mammal room that has consistent air flow, a temperature set between 20-23℃, and a diurnal cycle of 12h light/12h dark. Purina Labdiet 5001 was used as a maintenance diet and Purina Formulab diet 5008 was given when mice were used for breeding or experimental purposes. A veterinarian would evaluate the health of the mice at a regular weekly interval, while vivarium staff and Dr. Udan's lab personnel would provide an additional evaluation on a daily basis. Using the breeding protocol, mice were bred to expand the line. Mice having the following mutation, *myosin regulatory light chain 7* (*Myl7*$^{+/-}$), and on a CD1 background were bred and a colony maintained to ensure sufficient availability of mice for the study. Mice needed for this study were *Myl7*$^{+/-}$ females at an ideal age of 2-8 months, and *Myl7*$^{+/-}$ males at an ideal age of 2 months to one year. To collect embryos for experiments, a heterozygous *Myl7*$^{+/-}$ dam was bred with a heterozygous *Myl7*$^{+/-}$ stud. Plugs were checked daily and every morning. Presence of a plug in the afternoon would mark the female having embryos

that are at embryonic day (E) 0.5, and the pregnant female would then be humanely euthanized 10 days later to collect E10.5 mouse embryos for the project.

Embryo Collection and Genotyping

To collect embryos, pregnant dams were euthanized by CO_2 inhalation followed by cervical dislocation. Dissections were done to remove the uterus, and the uterus was moved to a Petri dish full of ice-cold phosphate buffer saline (PBS). Embryos were dissected out of the uterus, while keeping the yolk sac intact. At this point, the procedure would differ depending on whether embryos were used for isolating RNA from the yolk sac tissue (for quantitative polymerase chain reaction [qPCR] studies) or to prepare the embryos for cryosectioning and immunostaining. For qPCR studies, yolk sacs were isolated per embryo for the purposes of extracting RNA, while the corresponding embryos were used to determine the genotype of the respective yolk sacs. For the cryosection/immunostaining experiments, embryos were prepared for cryosectioning, while yolk sacs were used for genotype determination.

Genotyping was an important aspect of the study, as comparisons needed to be made between the control group (*Myl7*$^{+/-}$ embryo) and the experimental group (*Myl7*$^{-/-}$ embryo). The *Myl7* gene is an atrial specific myosin that is required for contractility of the atria of the heart. The null mutation does not result in a phenotype when heterozygous. However, homozygous mutant embryos have impaired heart contractility and poor blood flow. Thus, mutant embryos were used to determine the effect that poor blood flow has on the development of the embryonic vasculature. To genotype the embryos or yolk sacs, DNA was extracted from the relevant tissue. If extracting DNA from embryos, only a piece of the embryonic tail was required. If extracting DNA from yolk sacs, then the whole yolk sac was used. Regardless of the tissue type, samples

were placed in a microcentrifuge tube and treated overnight at 55°C with 200µL embryo lysis buffer (50mM Tris, [pH 8.0], 100mM EDTA, 0.5% SDS) with 8µL of Proteinase K. The next morning, phenol:chloroform:isoamyl alcohol reagent was added to each sample in a 1:1 ratio. Then, the microcentrifuge tubes were shaken up and down for 20-30 times until the solution turned white. Then, the tubes were centrifuged at a maximum speed of 13.3g for 10 minutes. Next, the aqueous phase of the tubes (top layer) was transferred in a clean microcentrifuge tube, and this was followed by precipitation of DNA with 100% isopropanol. After gently discarding the solution, the DNA pellet was washed with 70% ethanol and centrifuged 10 minutes at 13.3g. The ethanol was removed carefully, and tubes were dried at room temperature. The pellet was then suspended with 75-100µL of distilled water and kept at 4°C to use later.

The DNA was used to determine the genotype of each tissue by performing PCR. To determine presence of the mutation, the following primers were used: *Myl7* mutant forward primer (5'-3') ACAGGGAATCACA, *Myl7* mutant reverse primer (5'-3') CGAACCTGGTCGA. To determine the presence of the wild type version of the *Myl7* gene, the following primers were used: *Myl7* wild type forward primer (5'-3') GGCACGATCACTC, *Myl7* wild type reverse primer (5'-3') ATCCCTGTTCTGG. To prepare the sample for PCR, a 40 µL reaction mixture was prepared per sample by mixing 25µL of the Pro-Taq DNA polymerase master mix (Denville scientific Inc, CB-4065-4), with 4µL of the forward and reverse primers, 20µL of distilled water, and 1µL of genomic DNA. The PCR reaction was performed on a TECHNE thermocycler at the following conditions: 95°C for 5 minutes, followed by 35 cycles of 95°C for 30s, 56.5°C for 30s, and 72°C for 1 minute. At the end of the cycle, there was a final extension at 72°C for 5 minutes. Electrophoresis of the amplicon was done in a 2% agarose gel supplemented with 20µL of ethidium bromide and run at 100V. The Azure Biosystems c300 transilluminator and digital

imaging system was used to visualize the presence or absence of mutant and wild type bands in the respective samples.

qPCR

Obtaining Samples to Extract RNA. Yolk sacs were used to extract RNA. Yolk sacs are thin tissues that are only comprised of endoderm and mesoderm with substantial vascular structures. So, gene expression changes in yolk sacs usually denotes gene expression changes in the vasculature. Yolk sacs were collected by dissecting E10.5 mouse embryos. The dissection method is described above in the embryo collection and genotyping section. Six mutant and six wild type yolk sacs were used for RNA extraction. The respective tails of the embryos were used to determine the genotype of the yolk sacs.

RNA Extraction. RNA was extracted from yolk sacs using Qiagen RNeasy mini kit (cat. no. 74104) and following the company's instructions. Briefly, 400µL of RLT buffer supplemented with 4µL of β-mercaptoethanol (β-ME) was added to each yolk sac. Then, the yolk sacs were disrupted by pipetting. After centrifuging the lysate for 3 minutes at maximum speed, the supernatant was carefully transferred to a new microcentrifuge tube. Four hundreds micro liter of 70% ethanol was added to the tube and the mixture was then transferred into a RNeasy mini column which was placed into a 2 ml collection tube. This tube was then centrifuged for 15 secs at maximum speed. After, the flow-through was discarded. Subsequently, 350µL of RW1 buffer was poured into the RNeasy mini-column, centrifuged for 15 secs, and the flow-through was discarded after. The RNeasy mini column was then treated with a mixture of RDD buffer and DNase for 15 mins. To eliminate DNA nucleotides remaining on the column,

the column was subsequently washed first with the RW1 buffer then the RPF buffer using similar procedures as described above.

To extract RNA from the column, the RNeasy column was then placed in a new 2 ml collection tube and centrifuged for 1 min at maximum speed to dry the membrane. After drying, the RNA column was transferred to a new 1.5mL collection tube and 40µL RNase free water was pipetted directly onto the spin column. Finally, the tube was centrifuged for 1 min and the spin column was disposed of. The flow-through that has been collected at this point contains RNA, which was preserved at -80°C for further use.

Primer Design. Primer design involves multiple steps. At first, the sequence of the gene of interest for the qPCR study was obtained by using the Ensembl website (http://www.ensembl.org/index.html). The desired transcript was then selected and downloaded. After opening the document in Microsoft word, the exon was marked in red font. To minimize the amount of troubleshooting in the design of efficient primers (for PCR), the Thermo Fisher Scientific qPCR website was used to find the genomic map of efficient primers used by the company. Primers supplied by the Thermo Fisher company are verified for their efficiency, but these primers are expensive, and the sequence information is proprietary. However, the company does publish the approximate locations of these efficient primers (i.e., the exon-exon boundaries), and the predicted size of the PCR product made using a cDNA template. Thus, the sequence of these efficient primers can be deduced for each gene. Based on the exon-exon boundaries of the genomic map provided by Thermo Fisher Scientific, primers were designed from those exon sequences. Sequence information of these exon-exon boundary were used in the Primer 3 program/website (https://bioinfo.ut.ee/primer3-0.4.0/) and the parameters were adjusted to identify potential primers that span the intron and would produce a 50-125 bp amplicon from a

cDNA template. A successful design of primers would reveal various options of forward and reverse primers that would produce the correct amplicon. These primers were then validated subsequently. Further, these primers were tested in an in-silico PCR (UCSC in silico PCR) to ensure that they will not amplify other regions of the genome.

Primers were designed to detect different ECM and ECM-related genes. The forward and reverse primer sequence of those genes are described in Table 1.

Table 1: Primers used in my study

Primer Name	Forward primer	Reverse primer	Company name
Collagen -IVa	GAGAAGGCGCACAATCAAG	TGGATGTTGCAGTAGGCAAA	Invitrogen
MMP-9	TAATTGGGGCTGGCTTACAG	TCACACGCCAGAAGAATTTG	Eurofins
Lama1	CTAAGAATGGCGTCCTCCTG	CACCGTTGTTGACGTGAAAT	Eurofins
Fn	ATTTGCTCCTGCACGTGTTT	CAGGTCTACGGCAGTTGTCA	Eurofins
HsPg2	GCCTCTGTCAAGATGGCTTC	AGGTGCCACCATTCAGACAT	Eurofins
Lama 4	TGTTTGTTGGAGGTGTTCCA	AATTACAAAGTGGCGGATGC	Eurofins
Lamac1	GAAAGGCCAAAAACCTGTCA	AGGGAGCCTTCGATCTCATT	Eurofins
Nidogen-1	ATTCTCGCACAGGACAACCT	GTTCAGGCATTCTGCCCTAT	Eurofins
Nidogen-2	GGATGGCAGAGAGCTACAGG	CCACAGATGGAGGAGTCACA	Eurofins
PPIA	CACAAACGGTTCCCAGTTTT	TTCACCTTCCCAAAGACCAC	Eurofins
MMP-2	ACCCAGATGTGGCCAACTAC	GGTTTCAGGGTCCAGGTCAG	Eurofins
TIMP -1	GCGTACTCTGAGCCCTGCT	TCTCCAGTTTGCAAGGGATAG	Eurofins
TIMP-2	AGAAGAGCCTGAACCACAGG	GTCCATCCAGAGGCACTCAT	Eurofins

The next step was to check the primer validity by performing PCR and qPCR to determine whether the primers amplify one single amplicon or different amplicons. In PCR, primer validity was checked by using cDNA instead of genomic DNA. A master mix was prepared using the previously described PCR protocol. Two control samples were used, one without cDNA and another without primers to validate whether there are any mispriming events. Each PCR tube contained a 40µL reaction volume, and for control samples, the volume was adjusted with PCR grade water. The PCR was run following the parameters described above in genotyping section.

In the qPCR, primer validity was checked by using wild type cDNA as a sample. The master mix was prepared according to the qPCR protocol, and aliquoted to the appropriate well of a 96-well plate. The qPCR was run following the parameters described below in the qPCR section. The melt curves and CT values were used to determine which primers could be used for the experiment.

cDNA Synthesis. For the qPCR experiments, a two-step system was used, and as such, the cDNA was synthesized in the first step. The protocol for cDNA synthesis was followed from Promega's GoScript reverse transcriptase system (Promega: A5000). To synthesize cDNA, the RNA concentration for each sample was measured using the Qubit RNA BR assay kit (Invitrogen, REF: Q10210) and the Qubit 3.0 fluorometer (Company: Invitrogen, Catalog Q33216). After determining the RNA concentration for each sample, the next phase of the experiment (cDNA synthesis) took place using the Promega GoScript Reverse Transcriptase kit and protocol (Promega: Cat #A60001). Briefly, to ensure that all samples result in a similar cDNA concentration, the RNA concentrations of each cDNA synthesis reaction were adjusted to the same concentration, and q.s. to a total volume of 8µL per PCR tube. To each RNA sample,

1µL of random primer, and 1µL of oligo(dt) primer was added, yielding a final volume of 10µl per tube (first reaction mix). PCR tubes were run in a thermal cycler at 70°C for 5 mins followed by 4°C for 5 mins. For each sample, 10µL of the reverse transcription reaction mix (1.5µL of nuclease free water, 4µL Go-Script 5X reaction buffer, 2.0µL $MgCl_2$, 1µLPCR nucleotide mix, 0.5µL Recombinant RNasin Ribonulease inhibitor and 1µL GoScript Reverse Transcriptase) was made and placed on ice. Upon completion, 10µL of the reaction mix was combined with 10µL of the first reaction mix. This was then placed in a thermal cycler for another reaction at 25°C for 5 mins, 42°C for 1 hour, and 70°C for 15 mins. The mixture was aliquoted in a new microcentrifuge tube and kept at -80°C for further use.

The cDNA concentration was measured in Qubit 3.0 fluorometer by using Qubit ssDNA assay kit (Invitrogen by Thermo Fisher Scientific).

qPCR Procedure. The qPCR experiment was done to see the change of ECM expression in high-flow versus low-flow vessels (i.e., yolk sac tissues). A qPCR plate was designed using the Thermo Fisher Scientific software. Peptidylprolyl isomerase A (PPIA) which catalyzes protein folding was used as housekeeping gene and to conduct this test, cDNA was diluted according to the concentration of cDNA. Diluted cDNA was carefully added in the appropriate well in the 96 well plate. Each cDNA sample had a reference standard which is called technical replicate. The total 40 µL of qPCR master mix (GoTaq qPCR master mix, 2x 25µL, 13µL water, total primer 2µL) was prepared for each 10µL cDNA. The master mix was combined with each 10µL cDNA template and centrifuged briefly to mix properly. The qPCR reaction was performed using the QuantStudio 6 pro Real-time PCR system under the following conditions: 1 cycle of polymerase activation at 95°C for 2 minutes, 40 cycles of denaturation at 95°C for 15 secs followed by 40 cycles of annealing/extension at 60°C for 1 minute, and the

final step is 1 cycle of dissociation at 60°C. After completion of the test, qPCR data was transferred to a personal Thermo Fisher account via a cloud-based system.

Data Analysis

Data analysis was done by using Microsoft Excel software. CT values were taken to calculate gene expression change by using $2^{-\Delta\Delta Ct}$ method (Pfaffl, 2001). Student's t-test was used to determine any gene expression change between reduced versus normal flow yolk sacs.

Cryo-sectioning

Embryos were processed in different steps to perform Cryosectioning. At first, tissues were fixed 1 hour in 4% paraformaldehyde (PFA) at room temp (RT) followed by washing 4x10 mins each in PBS at 4 deg. The next step was dehydrating the embryos in 15% sucrose at 4°C overnight (O/N), and then embedding the embryos in 30% sucrose at 4°C O/N. Then, embryos were prepared for optical cutting temperature (OCT) penetration by submerging in 1:1 30%/OCT for 6 hours, and again in 1:2 30% sucrose /OCT for 6 hours at 4°C. Finally, an OCT block was prepared by embedding embryos in OCT on dry ice. Embryo sections (10µm) were prepared from the OCT blocks using a cryostat (Leica CM1860 UV) set at -26°C and placed onto poly-lysine coated positively charged slides. Slides were dried at RT for 6 hours and preserved at -80°C to use for immunostaining later.

Immunostaining

For immunostaining, slides were post-fixed in 4% PFA for 10 mins at RT. Slides were marked with PAP pen followed by washing 4 times for 10 mins each with PBT (phosphate

buffered saline with 0.1% Triton X-100). Then, samples were blocked in a blocking solution for 1 hour at RT. The blocking solution was prepared with 2% of normal donkey serum (NDS) in PBT. Samples were then incubated with primary antibody overnight at 4°C.

Slides were washed 4 times with PBT 10 mins each at RT. After washing, slides were incubated in secondary antibody for 1 hour at RT followed by 4 times washing with PBT 10 mins each at RT. Excess PBT was wiped from around the specimen and samples were mounted with flourmount (Sigma-Aldrich, f6182). A coverslip was added to each slide and stored at 4°C for imaging later. Primary and secondary antibodies used in this procedure are listed in Table 2.

Table 2: Antibody's used in this study.

Antibody	Dilution	Company	Incubation period
Anti-vascular endothelial growth factor Receptor-2 (primary antibody), made in goat	1:200	SIGMA	24 hours
Collagen-4 antibody (primary), made in rabbit.	1:500	BIO RAD	24 hours
MMP-9 antibody (primary)	1:500	BIO RAD	24 hours
Alexa flour 488 donkey anti-goat	1:500	Invitrogen	1 hour
Alexa 568 donkey anti-rabbit	1:500	Invitrogen	1 hour

Imaging

Imaging of the immuonstained frozen sections was done on the Olympus IX81-ZDC inverted confocal microscope and imaging data were collected using the Slidebook 6.0 program

as the computer interface. Images were taken using the Olympus 40xUPlanSApo objective, 20xLUCPlanFLN (NA 0.45) objective, and 10xUPlanSApo (NA 0.4). Images were collected using Hamamatsu EM-CCD digital camera and a 3i laser at 488nm and 561nm. Green and red fluorescence intensity was set to 100, averaging was set to 8 and the exposure time was 50ms. Different regions of the samples were imaged to find out basement membrane deposition for both Collagen-IVa and MMP-9.

RESULTS

Hemodynamic Force Modulates the Expression of ECM Genes

In previous studies in the Dr. Udan's lab, it was determined that hemodynamic force regulates recruitment and attachment of vSMCs from neighboring low-flow vessels to the dominant high-flow vessel present within the developing yolk sac. But what has remained unknown is the molecular mechanism that supports the attachment of migratory/unattached vSMCs specifically to the high-flow vessel, as opposed to the low-flow vessels that the vSMCs encounter during their migration. To explain this phenomenon, one hypothesis was formulated: hemodynamic force modulates the expression of ECM and ECM-modifying genes to form a thick basement membrane (BM) that enhances the attachment of vSMCs in high-flow vessels. Formation of a thick BM on the abluminal side of the vessel (the side of the endothelium tissue that does not contact blood flow) may cause the vessel to be more adhesive to extramural cells (cells that surround vessels). Hence, any high-flow vessels present in the developing yolk sac would have a thick BM, whereas the low-flow vessels would have a thin BM. This would favor the unattached migratory vSMCs to specifically attach to the high-flow vessels.

To determine whether hemodynamic force regulates the expression of ECM or ECM-modifying genes, I compared the gene expression of normal-flow yolk sacs (i.e., *Myl7*$^{+/-}$ yolk sacs that contains mostly blood vessels having a diversity of blood flow—(low- and high-flow vessels) with that of reduced-flow yolk sacs (i.e., *Myl7*$^{-/-}$ yolk sacs that contain mostly blood vessels having very low to absent blood flow). Since the yolk sac is a simple tissue comprised of a double sheet of tissues (endoderm and mesoderm) that houses an extensive vasculature, I expect that gene expression analysis will allow us to detect any differences in vessels exposed to normal blood flow versus those exposed to reduce blood flow. The ECM genes that I sought to

evaluate were the following: *Collagen-4*, *Laminin1 alpha*, *Fibronectin*, *Lama4*, *Lamac1*, *Hspg2*, *Nidogen 1*, *Nidogen-2*. The products of these genes are deposited in the ECM to form the basement membrane in the abluminal side of the vessel. I also wanted to evaluate whether blood flow affected expression of ECM-modifying genes. These genes are those whose protein products physically modulate the ECM by either breaking the ECM down (*matrix metalloproteinases* [*MMPs*]) or genes that inhibit the function of enzymes that degrade the matrix (*tissue inhibitors of MMPs known as TIMPs*). Though *MMPs* and *TIMPs* are a rather large family of genes, I sought to evaluate those that are known to be expressed specifically in the endothelium: *MMP-9*, *MMP-2*, *TIMP-1*, and *TIMP-2*.

Assessment of ECM gene expression differences in reduced-flow yolk sacs by qPCR revealed no difference in the expression of *Fibronectin*, *Lama4*, *LamaC*, *Laminin 1 alpha*, *Nidogen 1*, and *Nidogen 2* (Figure 1). However, to my surprise, there was an increase in the expression of *Collagen IVa*. The upregulation was significant, resulting in a ~ 3.75X (which is a very large amount of change that is not common for these altered flow studies). In addition to the *Collagen IVa* result, there was also a slight increase in *Hspg2*. Both of these were unexpected results, as I posited that decreased blood flow would result in blood vessels secreting a thinner ECM. Gene expression changes are calculated by CT value. CT values are mentioned in Table 3.

To assess whether reduced-flow causes the vessels to deposit less ECM of the BM, perhaps flow regulates the expression of ECM-modifying genes. This category of genes includes *Matrix metalloproteinases (MMPs)* that enhance breakdown of the ECM, or *TIMPs (Tissue inhibitor of matrix metalloproteinases*) that act to inactivate *MMPs*. From my analysis, I determined that *TIMP-1* is upregulated 1.5 fold in reduced-flow embryos, and there was a

dramatic upregulation in one of the two endothelial *MMPs—MMP-9* (Figure 2) Thus, in the reduced-flow yolk sacs, *MMP-9* was upregulated by 5.5X.

Table 3: CT values for ECM and ECM related genes in control and experimental samples in the qPCR study.

Name of the genes	Average CT value for Mutant reduced-flow samples	Average CT values for Normal-flow control samples	Average CT values for housekeeping gene PPIA for mutant samples	Average CT values for housekeeping gene PPIA for Normal-flow control samples
Fibronectin	22.10	22.13	17.49	17.56
Laminin	24.78	25.05	17.86	17.90
Collagen IVa	32.56	34.41	17.76	17.69
MMP-9	27.22	29.90	17.28	17.50
MMP-2	26.79	26.53	17.16	18.04
Hspg2	27.08	27.59	17.98	17.83
Lama4	26.76	27.22	18.44	18.46
Lamac1	24.08	24.36	18.08	18.13
Nidogen 1	30.15	31.12	17.97	17.93
Nidogen-2	24.33	24.65	17.65	17.51
TIMP-1	25.41	25.84	18.38	18.26
TIMP-2	29.01	28.74	18.48	18.62

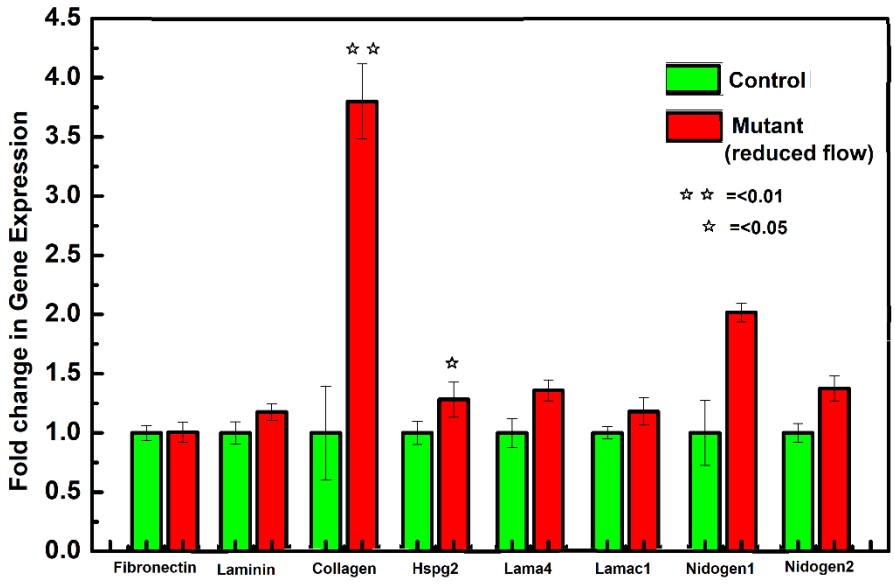

Figure 1: Change in ECM mRNA expression in reduced-flow vessel. *Collagen-IV* is 3.75x upregulated in reduced-flow yolk sacs. *Hspg2* is upregulated 1.25x in reduce-flow vessel. There is no significant change in other ECM genes expression due to low hemodynamic force. Statistical significance was calculated using standard error. Standard error is built into the result. Student's t-test was used. P-value <0.05 and <0.01 respectively.

Immunostaining Results

Based on the qPCR results, it is unclear how this affects BM formation in the reduced-flow vs normal-flow vessels of the yolk sac. Thus, the ideal way to make sense of these results is to assess the deposition of these proteins *in vivo*. I decided to use immunostaining to visualize Collagen IVa deposition (as well as MMP-9) around high-flow and low-flow vessels. For this study, the yolk sac vessels were not evaluated because the large high-flow vessels are very difficult to find amongst all other vessels of the yolk sac in a section, because it would remove morphological hallmarks found in the flat mounted yolk sacs. Thus, I decided to assess ECM deposition of the BM of the large dorsal aortae found within the embryo. I wanted to evaluate whether the immunostaining could be successful, thus I tested them out on wild type samples.

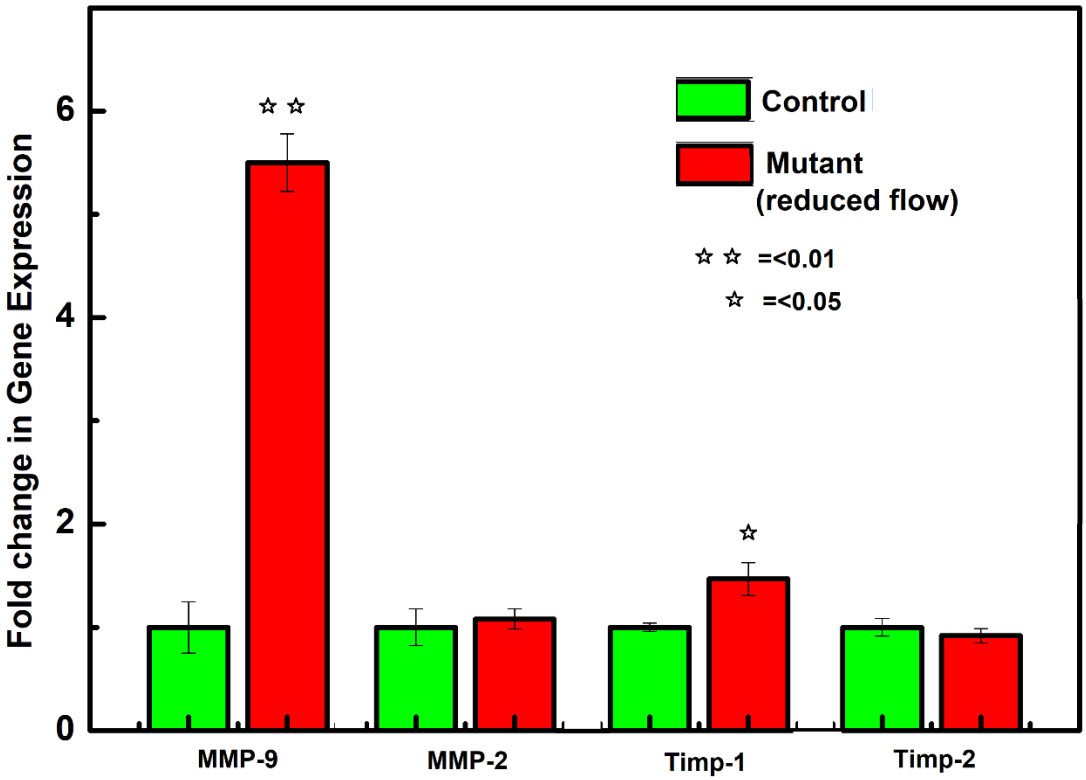

Figure 2: Change in ECM remodeling genes expression in reduced-flow vessel. *Mmp-9* is 5.5x upregulated in reduced-flow mutant vessel. There is no change in other ECM modifying genes due to low hemodynamic force. Statistical significance was calculated using standard error. Standard error is built into the result. Student's t-test was used. P-value <0.05 and<.01 respectively.

Collagen IVa is diffusely distributed throughout the tissue; however, particularly around the epithelial tissues (such as the endothelium of the dorsal aortae, as well as the epithelium of the foregut) where the Collagen IVa staining was very abundant and seemed to be located in a dense band where the BM is expected to be (Figure 3). My data provide evidence of Collagen IVa staining. The Collagen IVa staining did seem to be expressed at low levels in other tissues, which is to be expected for a widely expressed ECM gene. I did not use any primary antibody control. Flk1 is a cell membrane receptor tyrosine kinase also designated as VEGFR-2.

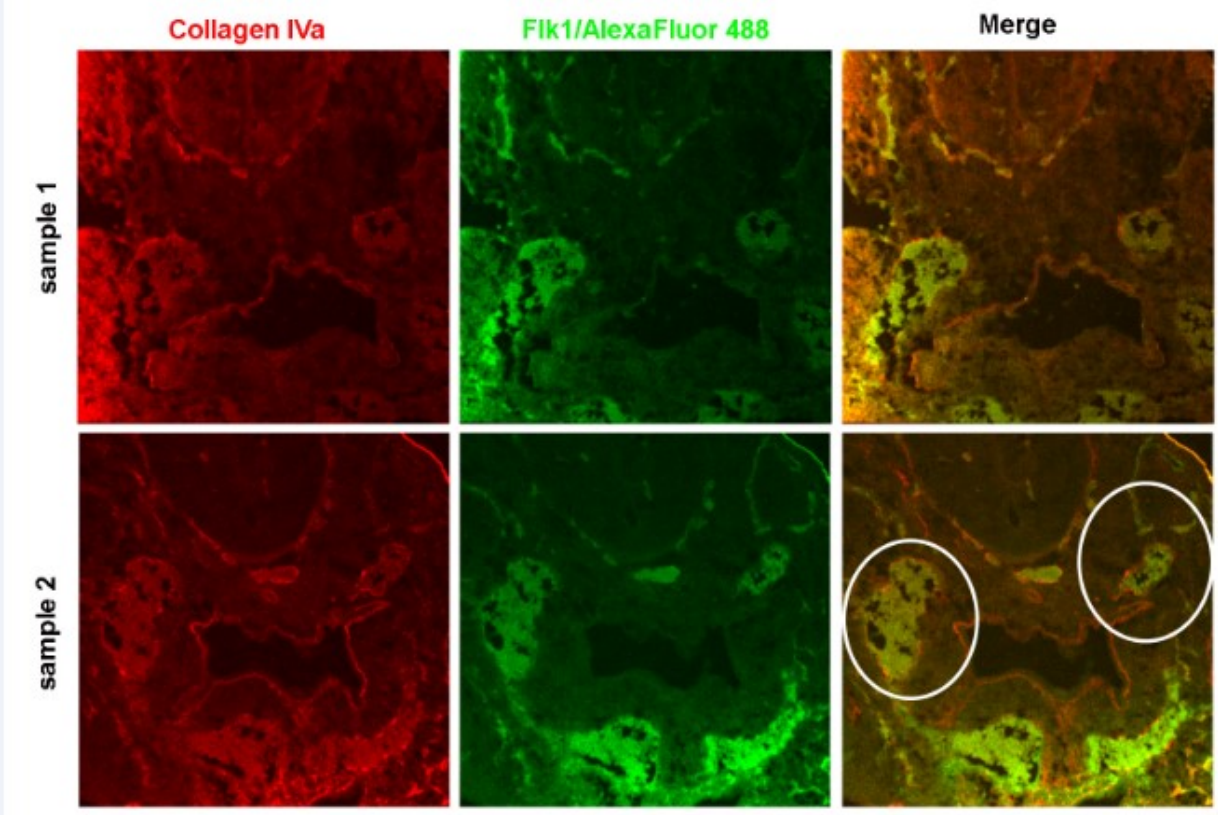

Figure 3: Dorsal Aorta cross section of normal-flow embryos were labeled with Flk1/AlexaFlour 488 and Collagen IVa antibody. Endothelium of dorsal aorta showing thick band of collagen in basement membrane. Collagen-IVa is also expressed in other structures at low level.

MMP-9 is also distributed in a similar manner in the BM of the endothelium of the dorsal aortae, and a little bit around the much smaller foregut. However, the staining appeared to be more diffuse a little further from the endothelium (green staining), which is to be expected for a secreted molecule (Figure 4). Also, MMP-9 seems to be expressed in other tissues, which is not unexpected, because it is not an endothelial-specific gene.

Another major issue that is very common when analyzing vessel cross sections in embryonic samples is the presence of blood cells, which are highly autofluorescent. Further, the fixation process can increase this autofluorescence. So, within the blood vessels there can be blood trapped inside, and that blood autofluorescence is present using both types of excitation

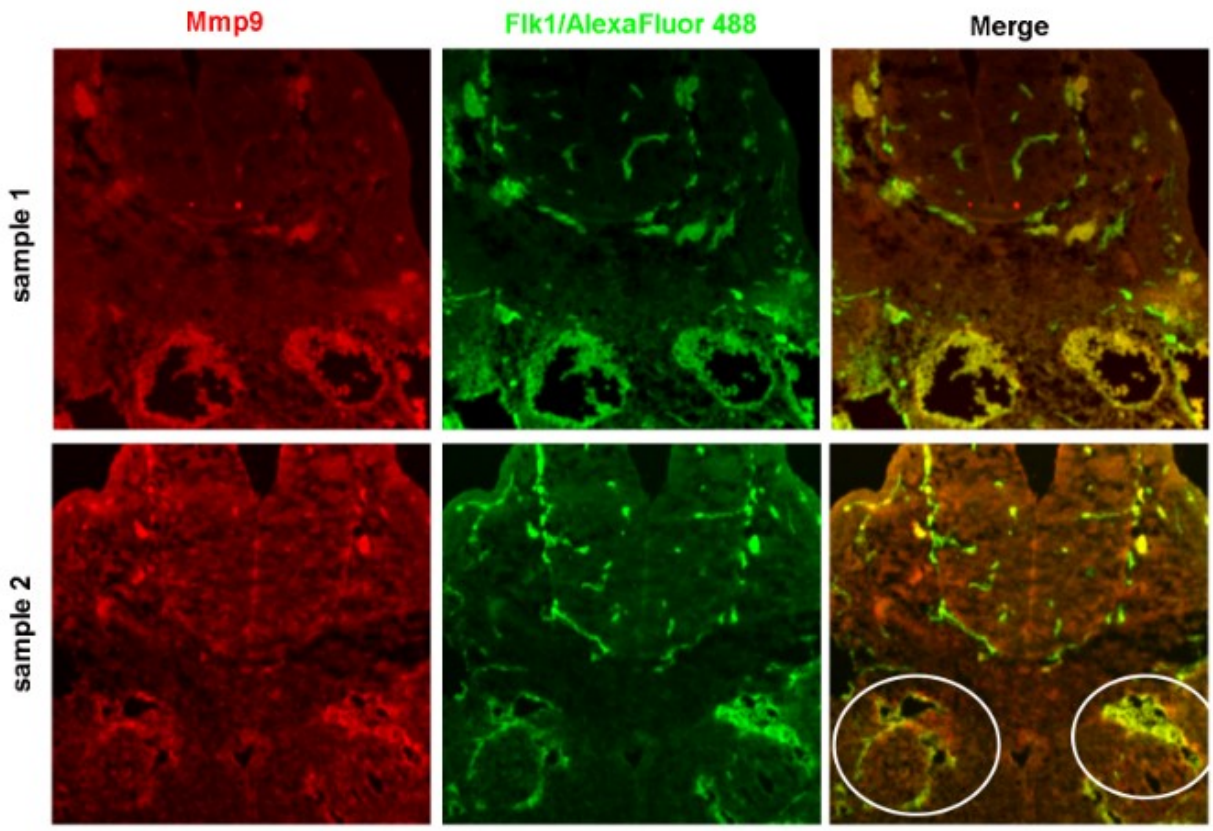

Figure 4: Dorsal Aorta cross section tissue of normal-flow embryos were labeled with Flk1/AlexaFlour488 and MMP-9 antibody. Mmp-9 staining is detected in the endothelium of dorsal aorta and to a lesser amount in the foregut. Other structures also are expressing MMP-9 at a low level.

lasers (488 nm and 561nm) resulting in enhanced red and green background staining inside the dorsal aortae (unless vessel sections lack blood).

The critical experiment, however, was to compare these stainings with that of *Myl7*$^{-/-}$ (reduced-flow embryos). But the mutant embryos we collected were decaying and we could not get appropriate samples to observe Collagen-IVa and MMP-9 deposition in the BM of dorsal aortae. Moreover, due to time restrains it was not possible to go for further embryo collection and processing. However, based on the qPCR data, I anticipate that the dorsal aortae of these embryos would exhibit high *MMP-9* expression.

With the *Collagen IVa* result, to support our hypothesis, I would expect to see that Collagen IVa would be downregulated in reduced flow. However, the qPCR data shows the opposite result. The ultimate goal would then be to determine whether this translates to protein levels.

DISCUSSION

The premise of this research study has been to determine the molecular mechanism governing the attachment of unattached/migratory vSMCs to proximal blood vessels exposed to high hemodynamic force/high blood flow. This process of blood vessel maturation is crucial to ensure that proximal vessels receive the appropriate thickness/coverage of the tunica media layer around blood vessels. A thicker coverage is not needed at the same degree in more distally located vessels that are exposed to lower hemodynamic force/low blood flow. This study was conducted to determine whether there are any changes in the gene expression pattern of ECM and ECM-modifying genes between high-flow versus low-flow vessels that may explain the formation of a thicker BM and more vSMCs attachment to high-flow vessels. The mechanism for how vSMCs attach to ECM proteins could be explained by integrin-mediated adhesion. Integrins are heterodimeric transmembrane proteins that promote vSMC-endothelial adhesion by binding to ECM proteins of the basement membrane located in the abluminal side of the blood vessel endothelium. Conditional knock-out studies showed that loss of integrin β1 prevents the attachment of vSMCs to endothelial cells (Abraham, Kogata, Fässler, & Adams, 2008). Thus, it seems that integrin-mediated adhesion is important for vSMC attachment. It was reported in another study that integrin α5β3 is required for vSMC attachment to the endothelial BM. Moreover, different ECM proteins like Collagen, Laminin, Fibronectin, Hspg2 can bind with different subunits of integrin receptor (Scheppke, Murphy, et al., 2012). I thus proposed a hypothesis that hemodynamic force may upregulate the expression of ECM genes or alter the expression of ECM-modifying genes that normally act to control ECM deposition in the BM to enhance the integrin- mediated vSMC adhesion to endothelial cells.

The qPCR experiments conducted in this study, comparing reduced-flow yolk sacs with normal-flow yolk sacs, revealed conflicting data. In support of the hypothesis, I observed an upregulation of *MMP-9* in reduced-flow yolk sacs, which may explain why low-flow vessels have less deposition of ECM proteins in the BM. However, conflicting results revealed an increase in *Collagen IVa* expression in reduced-flow yolk sacs, which does not fit with our hypothesis.

MMPs are tissue remodeling genes known to be expressed in many cell types, including in endothelial cells, and which act by degrading ECM proteins for different reasons such as to remodel repairing tissue, to promote immunological cell migration through tissues, and to promote changes in development. Thus, *MMPs* play an important role in modifying tissue development such as with the changes that take place during vasculogenesis and angiogenesis (Van Hinsbergh, Engelse, & Quax, 2006). I speculate that vessels exposed to reduced blood flow may upregulate expression of specific *MMPs* that are known to be expressed in the endothelium of blood vessels and downregulate expression of endothelially expressed *TIMPs*. By upregulating *MMPs*, this may enhance breakdown of the BM, while downregulation of *TIMPs* may enhance the function of *MMPs*. Interestingly, my results revealed that there was a 5.5 fold upregulation of *MMP-9* in the reduced-flow yolk sacs as compared to normal-flow yolk sacs. Though there was no change in expression *MMP-2*, the upregulation in *MMP-9* expression was significant and congruent with the hypothesis. Thus, MMP-9 may act to breakdown the ECM within low-flow vessels, much more so than in high-flow vessels that express a lower level of MMP-9. This may support the model that the endothelium of high-flow vessels has a thicker BM. But there was also a 1.5 fold upregulation of *TIMP-1* which is unexpected result because upregulation of *TIMPs* can downregulate *MMP-9*.

However, findings from this study also showed that *Collagen IVa* exhibited a ~ 3.75 fold upregulation in the reduced-flow yolk sacs. The observed upregulation is an unexpected result as increased Collagen IVa production and deposition should lead to enhanced adhesiveness of vSMCs to low-flow blood vessels. This result is opposite of the expectation. However, it is possible that the basement membrane deposition is still diminished in the reduced-flow yolk-sacs, but by another means such as modulating expression of ECM modifying genes, and the observed increased in *Collagen IVa* expression could be caused by a negative feedback loop. Hspg2 is also showed 1.25 fold upregulation in reduced-flow vessels which is also unexpected because upregulation of Hspg2 can help in thick BM formation, which is contrary to the hypothesis.

Since it is not possible to make a conclusion from these results based on gene expression changes alone, I then set off to perform immunostainings to qualitatively assess whether there is change in protein expression for Collagen-IV and MMP-9 around the dorsal aortae vessels between reduced-flow and normal-flow embryos. The benefit of immunostainings is that it not only allows for observing changes in protein levels (which do not always match with changes in RNA transcript levels), but it also provides resolution for determining where in the tissues any changes in these proteins will be found (preferably around the endothelium). As previously mentioned, due to time restrictions I was unable to assess Collagen IVa and MMP-9 protein expression in reduced-flow embryos but did observe both Collagen IVa and MMP-9 staining surrounding the endothelium in the region where the BM would be expected to be found. Upon completion of these experiments the final expectation is to observe a thick BM (Collagen-IVa*)* surrounding the dorsal aortae of normal-flow embryos, with a thinner BM around the dorsal aortae of reduced-flow embryos. Even though this result counters that of the observed changes in

Collagen-IVa mRNA levels, it is possible that hemodynamic force can modulate translational or post-translational mechanisms of gene regulation to encourage Collagen-IVa protein production (even upon diminished mRNA production). Regarding MMP-9 expression, I expect the opposite expression pattern, which is supported by the gene expression studies.

Other ECM proteins like Laminin, Fibronectin, Nidogen, Hspg2 may deposit around the dorsal aortae of the normal-flow embryos. Here, the mechanisms again could be translational or post-translational mechanisms of gene regulation that are coopted by hemodynamic force. Immunostainings also could be done with these ECM and ECM related proteins to see any difference in the protein expression.

In another model, it is possible that integrin-B1 (known to be expressed in vSMCs) is upregulated in vSMCs when they are in close proximity to high-flow vessels. It is likely that for this occur, the vessels must be receiving an unidentified paracrine factor that is upregulated by the endothelial cells of high-flow vessels. This paracrine factor might play a role to promote integrin-B1 expression and increase adhesiveness of local vSMCs to vessels that have a BM (even if the BM is not more thick). This could be tested by immunostaining.

Because *MMP-9* resulted in the highest-level increase in expression, in reduced flow yolk sacs, in future studies, it will be important to explore the role of this gene in vSMC attachment. Thus, future experiments could be exposing cultured mouse embryos with an Mmp9 inhibitor (such as an antagonist or a blocking antibody). Since MMP-9 would be expected to be expressed at a high level in the distal, low-flow capillary region of the yolk sac, then MMP-9 inhibitors may enhance attachment of the vSMCs to the distal capillaries, even in the normal-flow embryos

Though, this study will be regarded as basic science research, my findings could have important therapeutic implications. Understanding the role of ECM and ECM modifying genes

in BM formation could be used to manipulate vSMCs attachment to treat different vascular diseases. For example, vascular aneurysms are characterized by weakening and ballooning of vessel wall, partially caused by the depletion of tunica media that are susceptible to rupturing and hemorrhaging. Currently, endovascular stents are used to treat abdominal aortic aneurysms, however, many patients encounter recurrent aneurysm events, leading to a reduced life expectancy (Avishay, 2021). As stents can be seeded with drug to render localized treatment (García-García, Vaina, Tsuchida, & Serruys, 2006), stents could be seeded with ECM and ECM remodeling factors to promote attachment of vSMCs to the thin vessel walls to prevent further event. Moreover, knowledge gained from this study can be utilized in designing artificial vasculature in tissue-engineering field. For example, if endothelial BM formation is the key to enhance endothelial-vSMCs attachment, proximal vessel could be genetically modified by gene editing to promote expression of ECM genes or downregulate expression of *MMP* genes. In summary, my basic science research could pave the way of probable clinical advancement.

REFERENCES

Abraham, S., Kogata, N., Fässler, R., & Adams, R. H. (2008). Integrin β1 subunit controls mural cell adhesion, spreading, and blood vessel wall stability. *Circulation Research*, *102*(5), 562–570. https://doi.org/10.1161/CIRCRESAHA.107.167908

Amacher, A. L., & Drake, C. G. (1975). Cerebral artery aneurysms in infancy, childhood and adolescence. *Pediatric Neurosurgery*, *1*(1), 72–80. https://doi.org/10.1159/000119557

Anderson, R. H., Webb, S., Brown, N. A., Lamers, W., & Moorman, A. (2022). Development of the heart:(2) Septation of the atriums and ventricles. *Heart.Bmj.Com*. https://doi.org/10.1136/heart.89.8.949

Armulik, A., Abramsson, A., & Betsholtz, C. (2005). Endothelial/pericyte interactions. *Circulation Research*, *97*(6), 512–523. https://doi.org/10.1161/01.RES.0000182903.16652.D7

Avishay, D.,(2021), Abdominal Aortic Repair. *Ncbi.Nlm.Nih.Gov*. Retrieved from https://www.ncbi.nlm.nih.gov/books/NBK554573/

Buschmann, I., Pries, A., Styp-Rekowska, B., Hillmeister, P., Loufrani, L., Henrion, D., Le Noble, F. (2010). Pulsatile shear and Gja5 modulate arterial identity and remodeling events during flow-driven arteriogenesis. *Development*, *137*(13), 2187–2196. https://doi.org/10.1242/DEV.045351

Campinho, P., Vilfan, A., & Vermot, J. (2020). Blood Flow Forces in Shaping the Vascular System: A Focus on Endothelial Cell Behavior. *Frontiers in Physiology*, *11*. https://doi.org/10.3389/FPHYS.2020.00552

Collart, C., Ciccarelli, A., Ivanovitch, K., Rosewell, I., Kumar, S., Kelly, G., Smith, J. C. (2021). The migratory pathways of the cells that form the endocardium, dorsal aortae, and head vasculature in the mouse embryo. *BMC Developmental Biology*, *21*(1). https://doi.org/10.1186/S12861-021-00239-3

D'Alessio, A., Moccia, F., Li, J., (2015), Angiogenesis and vasculogenesis in health and disease. *Hindawi.Com*. Retrieved from https://www.hindawi.com/journals/bmri/2015/126582/

Eerola, I., Boon, L., Mulliken, J., (2003), Capillary malformation–arteriovenous malformation, a new clinical and genetic disorder caused by RASA1 mutations. *Elsevier*. Retrieved from https://www.sciencedirect.com/science/article/pii/S0002929707639779

Fang, J., & Hirschi, K. (2019). Molecular regulation of arteriovenous endothelial cell specification. *F1000Research*, *8*. https://doi.org/10.12688/F1000RESEARCH.16701.1

French, W. J., Creemers, E. E., & Tallquist, M. D. (2008). Platelet-Derived Growth Factor

Receptors Direct Vascular Development Independent of Vascular Smooth Muscle Cell Function. *Molecular and Cellular Biology*, *28*(18), 5646–5657. https://doi.org/10.1128/MCB.00441-08

García-García, H. M., Vaina, S., Tsuchida, K., & Serruys, P. W. (2006). Drug-eluting stents. *Archivos de Cardiologia de Mexico*, *76*(3), 297–319. https://doi.org/10.1161/circulationaha.106.646190

Garcia, M. D., Lopez, A. L., Larin, K. V., & Larina, I. V. (2015). Imaging of cardiovascular development in mammalian embryos using optical coherence tomography. *Methods in Molecular Biology*, *1214*, 151–161. https://doi.org/10.1007/978-1-4939-1462-3_8

Jain, R. K. (2003). Molecular regulation of vessel maturation. *Nature Medicine*, *9*(6), 685–693. https://doi.org/10.1038/NM0603-685

Jayroe, H., (2020) Arteriovenous fistula. *Ncbi.Nlm.Nih.Gov*. Retrieved from https://www.ncbi.nlm.nih.gov/books/NBK559213/

Jones, E. A. V., Yuan, L., Breant, C., Watts, R. J., & Eichmann, A. (2008). Separating genetic and hemodynamic defects in neuropilin 1 knockout embryos. *Development*, *135*(14), 2479–2488. https://doi.org/10.1242/DEV.014902

Lawson, N., Scheer, N., Pham, V., Kim, C., & Chitnis, A. (2001). Notch signaling is required for arterial-venous differentiation during embryonic vascular development. Retrieved from https://journals.biologists.com/dev/article-abstract/128/19/3675/41372

le Noble, F., Moyon, D., Pardanaud, L., Yuan, L., Djonov, V., Matthijsen, R., Eichmann, A. (2004). Flow regulates arterial-venous differentiation in the chick embryo yolk sac. *Development*, *131*(2), 361–375. https://doi.org/10.1242/DEV.00929

Levy, M., Levy, D., (2021), . Pediatric cerebral aneurysm. *Ncbi.Nlm.Nih.Gov*. Retrieved from https://www.ncbi.nlm.nih.gov/books/NBK537085/

Lindblom, P., Gerhardt, H., Liebner, S., Abramsson, A., Enge, M., Hellström, M., Betsholtz, C. (2003). Endothelial PDGF-B retention is required for proper investment of pericytes in the microvessel wall. *Genesdev.Cshlp.Org*. https://doi.org/10.1101/gad.266803

Lucitti, J. L., Jones, E. A. V., Huang, C., Chen, J., Fraser, S. E., & Dickinson, M. E. (2007). Vascular remodeling of the mouse yolk sac requires hemodynamic force. *Development*, *134*(18), 3317–3326. https://doi.org/10.1242/DEV.02883

Majesky, M. W. (2018). Vascular development. *Arteriosclerosis, Thrombosis, and Vascular Biology*, *38*(3), E17–E24. https://doi.org/10.1161/ATVBAHA.118.310223

Mathew, P., (2021), Embryology, heart. *Ncbi.Nlm.Nih.Gov*. Retrieved from https://www.ncbi.nlm.nih.gov/books/NBK537313/

Oliver, G., & Srinivasan, R. S. (2010). Endothelial cell plasticity: How to become and remain a lymphatic endothelial cell. *Development*, *137*(3), 363–372. https://doi.org/10.1242/DEV.035360

Padget, R., Mohite, S., (2019), Hemodynamic force is required for vascular smooth muscle cell recruitment to blood vessels during mouse embryonic development. *Elsevier*. Retrieved from https://www.sciencedirect.com/science/article/pii/S0925477318301205

Paige, S. L., Plonowska, K., Xu, A., & Wu, S. M. (2015). Molecular regulation of cardiomyocyte differentiation. *Circulation Research*, *116*(2), 341–353. https://doi.org/10.1161/CIRCRESAHA.116.302752

Patan, S. (2004). Vasculogenesis and angiogenesis. *Cancer Treatment and Research*, *117*, 3–32. https://doi.org/10.1007/978-1-4419-8871-3_1

Pfaffl, M. W. (2001) A new mathematical model for relative quantification in real-time RT–PCR. *Academic.Oup.Com*. Retrieved from https://academic.oup.com/nar/article-abstract/29/9/e45/2384081

Ferrara, N. (2000), Vascular endothelial growth factor and the regulation of angiogenesis. *Europepmc.Org*. Retrieved from https://europepmc.org/article/med/11036931

Reynolds, M. R., Lanzino, G., & Zipfel, G. J. (2017). Intracranial Dural Arteriovenous Fistulae. *Stroke*, *48*(5), 1424–1431. https://doi.org/10.1161/STROKEAHA.116.012784

Ricard, N., & Simons, M. (2015). When It Is Better to Regress: Dynamics of Vascular Pruning. *PLoS Biology*, *13*(5). https://doi.org/10.1371/JOURNAL.PBIO.1002148

Risau, W., & Flamme, I. (1995). Vasculogenesis. *Annual Review of Cell and Developmental Biology*, *11*, 73–91. https://doi.org/10.1146/annurev.cb.11.110195.000445

Scheppke, L., Murphy, E., Blood, A. Z.-,(2012), Notch promotes vascular maturation by inducing integrin-mediated smooth muscle cell adhesion to the endothelial basement membrane. *Ashpublications.Org*. Retrieved from https://ashpublications.org/blood/article-abstract/119/9/2149/30239

Shalaby, F., Janet, R., Yamaguchi, T. P., Gertsenstein, M., Wu, X. F., Breitman, M. L., & Schuh, A. C. (1995). Failure of blood-island formation and vasculogenesis in Flk-1-deficient mice. *Nature*, *376*(6535), 62–66. https://doi.org/10.1038/376062A0

Suluba, E., Shuwei, L., Xia, Q., & Mwanga, A. (2020). Congenital heart diseases: genetics, non-inherited risk factors, and signaling pathways. *Egyptian Journal of Medical Human Genetics*, *21*(1). https://doi.org/10.1186/S43042-020-0050-1

Udan, R. S., Culver, J. C., & Dickinson, M. E. (2013). Understanding vascular development.

Wiley Interdisciplinary Reviews: Developmental Biology, *2*(3), 327–346. https://doi.org/10.1002/WDEV.91

Udan, R. S., Vadakkan, T. J., & Dickinson, M. E. (2013). Dynamic responses of endothelial cells to changes in blood flow during vascular remodeling of the mouse yolk sac. *Development (Cambridge)*, *140*(19), 4041–4050. https://doi.org/10.1242/DEV.096255

Van Hinsbergh, V. W. M., Engelse, M. A., & Quax, P. H. A. (2006). Pericellular proteases in angiogenesis and vasculogenesis. *Arteriosclerosis, Thrombosis, and Vascular Biology*, *26*(4), 716–728. https://doi.org/10.1161/01.ATV.0000209518.58252.17

Tuomas, T., et al. (2011) "VEGFR-3 controls tip to stalk conversion at vessel fusion sites by reinforcing Notch signalling." Nature cell biology 13.10: 1202-1213. https://doi.org/10.1038/ncb2331

Yousif, L., Russo, J. Di, (2013). Laminin isoforms in endothelial and perivascular basement membranes. *Taylor & Francis*, *7*(1), 101–110. https://doi.org/10.4161/cam.22680

APPENDIX: IACUC APPROVAL

April 18, 2022

RE: IACUC protocol 2020-21 and 2020-22

Hello Israt Jahan,

IACUC protocol #2020-21 entitled "Breeding protocol for the 'blood vessel maturation and heart morphogenesis' project" and 2020-22 "Blood vessel maturation and heart morphogenesis" were approved for 10/16/2020 to 10/15/2023 and you are an approved member on the protocols.

Thank you and if you need anything in the future regarding this protocol, please contact me either via email (Johnnapedersen@missouristate.edu) or at 417-836-3737.

Sincerely,

Johnna Pedersen